Electronic Supplementary Information (ESI) for

Chalcogen Bonding Interactions Between Ebselen and Nitrite Promote *N*-nitrosation of Amine

Tuhin Sahana,[a] Adwaith K. Valappil,[a] and Subrata Kundu*[a]

[a]School of Chemistry, Indian Institute of Science Education and Research Thiruvananthapuram (IISER-TVM), Thiruvananthapuram 695551, India

*Corresponding author email: skundu@iisertvm.ac.in, skundu.chem@gmail.com

1.   General Considerations and Physical Methods

All reactions were performed using anhydrous solvents under the inert atmosphere of an MBraun glovebox. NMR spectra were recorded on a Bruker Advance III 500 MHz NMR spectrometer at room temperature unless otherwise noted. The proton chemical shift (δ) values are expressed in ppm relative to tetramethylsilane, whereas the residual ^1H, ^{13}C signals of the deuterated solvent served as an internal standard. The ^{77}Se chemical shifts are reported in parts per million (δ) referenced to sodium selenite in D_2O at 1272 ppm as the external standard. High-resolution mass spectra (HRMS) were recorded on Thermo Scientific™ Q Exactive™ Hybrid Quadrupole-Orbitrap Mass Spectrometer using the electrospray ionization (ESI) technique.

2.   Materials

All chemicals were purchased from standard vendors (*e.g.* Sigma-Aldrich, Spectrochem, TCI) and used without further purification unless otherwise mentioned. Molecular sieves (4Å, 4–8 mesh beads) were activated in *vacuo* at 220 °C for 24 h. Anhydrous solvents were sparged with nitrogen and stored over activated molecular sieves under a nitrogen atmosphere. 2-phenyl-1,2-benzisoselenazol-3(2H)-one (commonly known as Ebselen) (**EbSe**) was purchased from TCI and 2-(4-methylphenyl)-1,2-benzisothiazol-3(2H)-one (**EbS**) was purchased from BLD Pharmatech.

3.   Computational Details

Density Functional Theory (DFT) calculations were carried out using Gaussian 16[S1] program package to optimize the structures, find the vibrational frequencies, and also the reaction enthalpies. The B3PW91 functional in conjunction with the 6-311G(2df,p) basis set was used for all the calculations.[S2,S3] Visualization, structural and molecular orbital (MO) analyses were performed using GaussView 06,[S4] Avogadro,[S5] CCDC Mercury[S6] and Chimera[S7]. All the ground state minima were confirmed by the absence of imaginary frequency. The solvent phase calculations were carried out using Solvent Model Density (SMD)[S8] model in chloroform solvent. The DFT-optimised cartesian coordinates are available in Table S3–S5.

4. Binding of NO_x^- (x = 2,3) Anions to Ebselen

General Procedure for ^{77}Se and ^1H NMR Titration

Ebselen **EbSe** (0.010 g, 0.036 mmol) was dissolved in anhydrous CDCl$_3$ (1.0 mL), and the solution was transferred to a sealed NMR tube under an inert atmosphere of a glovebox. ^{77}Se and ^1H NMR resonances of the authentic sample of **EbSe** were recorded in the absence of the guest molecule (0.00 equiv). Eighteen different vials were charged with calculated amount of tetra-*n*-butylammonium nitrite [Bu$_4$N][NO$_2$], as listed in Table S1. The above-mentioned **EbSe** solution (1.0 mL, 36.47 mM) in CDCl$_3$ was transferred to the first vial containing [Bu$_4$N][NO$_2$] under an argon atmosphere. Subsequently, ^{77}Se and ^1H NMR were recorded at room temperature. The same NMR sample solution along with the solution from the first vial, was transferred to the second vial containing [Bu$_4$N][NO$_2$]. The resultant solution was again analyzed by ^{77}Se and ^1H NMR. Likewise, the changes in the chemical shifts ($\Delta\delta$) of the ^{77}Se nucleus and different aromatic CH protons of **EbSe** were monitored each time upon sequentially increase in the concentration of [Bu$_4$N][NO$_2$] ranging from 0.00 mM to 318.92 mM (Figures 3-4). The association constant was determined from non-linear curve fitting for 1:1 host-guest complex using the Nelder-Mead method in Bindfit, an online tool for supramolecular chemistry research and analysis.[S9]

Similarly, ^{77}Se and ^1H NMR were monitored upon the addition of **EbSe** (1.0 mL, 36.47 mM) in CDCl$_3$ to different concentrations of tetrabutylammonium nitrate [Bu$_4$N][NO$_3$] ranging from 0.00 mM to 233.19 mM (Figures S12-S13).

The binding analysis of nitrite anion in [Bu$_4$N][NO$_2$] with **EbS** was carried out analogously using ^1H NMR analysis of **EbS** sample in the presence of varied concentrations of nitrite anion.

5. Nitrosation of Amine by Nitrite Anion in the Presence of EbE (E=Se/S)

Individual stock solutions of [Bu$_4$N][NO$_2$] (0.025 g, 0.087 mmol), (*p*-tolyl)$_2$NH (0.017 g, 0.087 mmol), **EbSe** (0.005 g, 0.018 mmol), and **EbS** (0.005 g, 0.020 mmol) were prepared by dissolving each compound in 1000 μL, 1000 μL, 1100 μL, and 1200 μL dichloromethane, respectively. These stock solutions were used for the reactions of amine, as described below.

For a representative stoichiometric reaction, [Bu$_4$N][NO$_2$] solution (200 μL stock solution, 0.017 mmol) and (*p*-tolyl)$_2$NH solution (200 μL stock solution, 0.017 mmol) were added to the solution of **EbSe** (1000 μL stock solution, 0.016 mmol) in a vial under an inert atmosphere of a glove box. The mixture was then diluted by adding dichloromethane (1.6 mL). The resultant

solution was allowed to stir at room temperature for 12 hours. Subsequently, the reaction mixture was dried in *vacuo* to afford a pale-yellow residue,.which was analysed by ^{1}H NMR. The relative integration of the proton resonances corresponding to the methyl groups in unreacted (*p*-tolyl)$_2$NH and (*p*-tolyl)$_2$N-NO provided the NMR spectroscopic yield (Table 1 and Figure S18). ^{1}H NMR (500 MHz, CDCl$_3$) of (*p*-tolyl)$_2$N-NO: δ 7.32-7.28 (m, 4H), 7.23 (d, 2H), 6.96 (d, 2H), 2.42 (s, 3H), 2.40 (s, 3H). ^{1}H NMR (500 MHz, CDCl$_3$) of unreacted (*p*-tolyl)$_2$NH: δ 7.06 (d, 4H), 6.95 (d, 4H), 2.29 (s, 6H). These proton resonances are comparable to that of the previous report.[S10]

For a representative catalytic reaction, the solution of **EbSe** (100 μL stock solution, 0.0016 mmol) was added to the equimolar mixture of [Bu$_4$N][NO$_2$] (200 μL stock solution, 0.017 mmol) and (*p*-tolyl)$_2$NH (200 μL stock solution, 0.017 mmol) in a vial under an inert atmosphere of a glove box. The mixture was then diluted by adding dichloromethane (2.5 mL) to maintain the same concentration of the reagents as that of in stoichiometric reaction. The resultant solution was allowed to stir at room temperature for 12 hours. Subsequently, the reaction mixture was dried in *vacuo* to afford a pale-yellow residue,. which was analysed by ^{1}H NMR (Table 1 and Figure S19).

The experiments with **EbS** were also carried out using analogously under the identical reaction conditions (Figures S18-S19).

For a control experiment, the reaction mixture of [Bu$_4$N][NO$_2$] (200 μL stock solution, 0.017 mmol) and (*p*-tolyl)$_2$NH (200 μL stock solution, 0.017 mmol) in dichloromethane (3.0 mL) was allowed to stir at room temperature for 12 hours. The resultant reaction mixture was analysed by ^{1}H NMR for comparison (Figure S18).

Comment*: While the generation of hydroxide anion (OH$^-$) based on the reaction stoichiometry has been proposed (Figure 2B), the characterization of OH$^-$ in solution was challenging.*
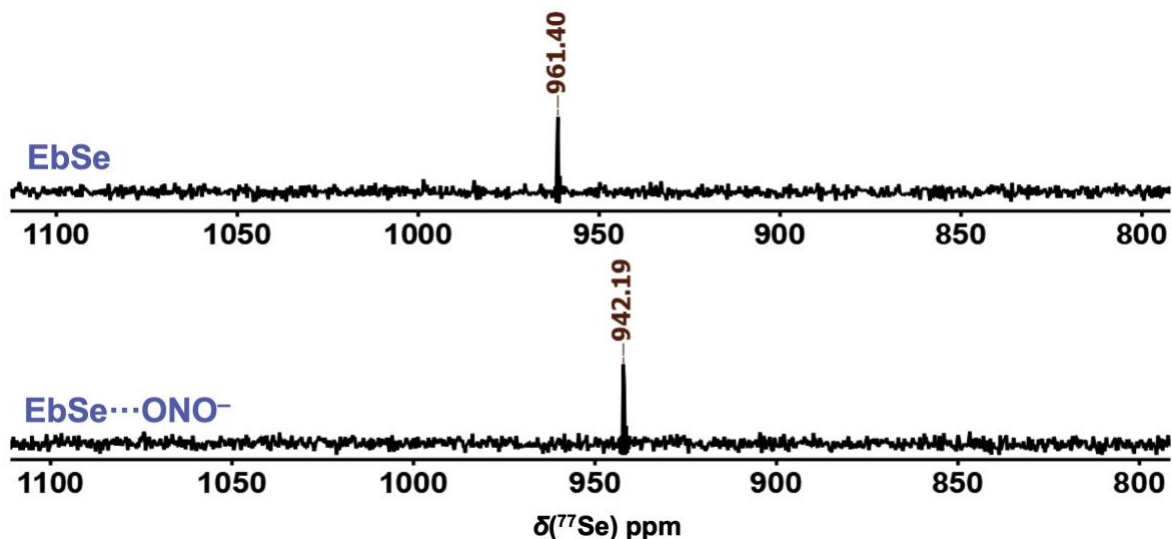
6.   Figures

Figure S1. ^{77}Se NMR (95 MHz, CDCl$_3$) of **EbSe** (top) and **EbSe···ONO⁻** (bottom). The NMR sample was prepared by dissolving **EbSe** (0.010 g, 0.036 mmol) and [Bu$_4$N][NO$_2$] (0.010 g, 0.036 mmol) in CDCl$_3$.
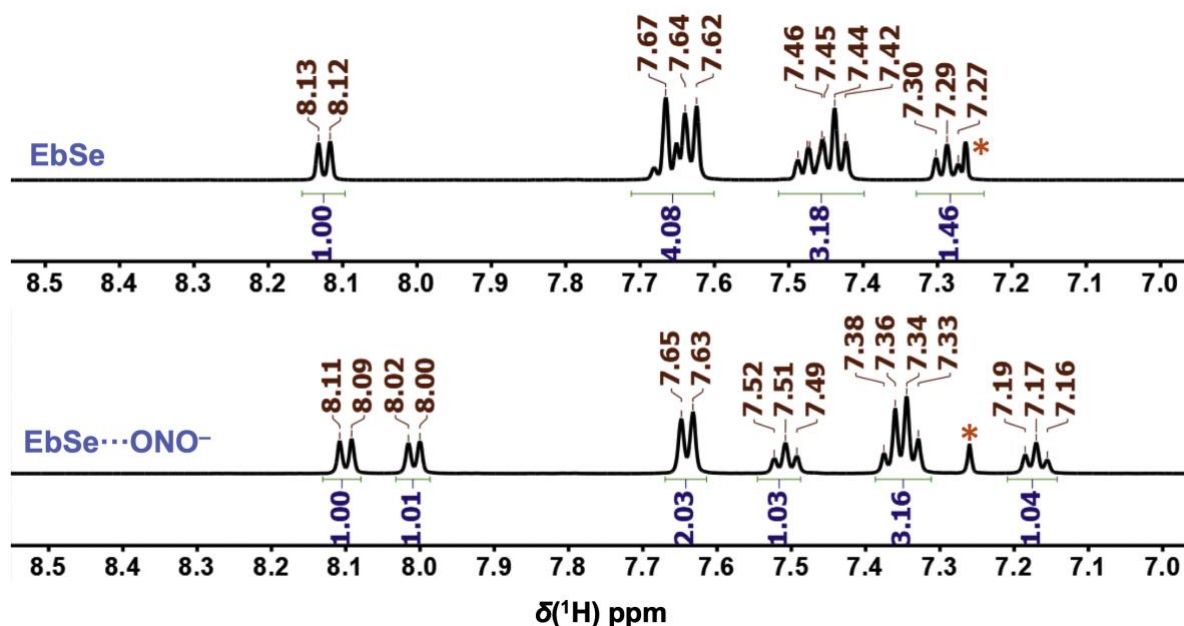

Figure S2. ^{1}H NMR spectra (500 MHz, CDCl$_3$) of **EbSe** (top) and **EbSe···ONO⁻** (bottom). The NMR sample was prepared by dissolving **EbSe** (0.010 g, 0.036 mmol) and [Bu$_4$N][NO$_2$] (0.010 g, 0.036 mmol) in CDCl$_3$. The aliphatic region of the bottom spectrum shows proton resonances for Bu$_4$N⁺ and is not shown for clarity. The peak marked with * originates from the solvent residual peak of CDCl$_3$.
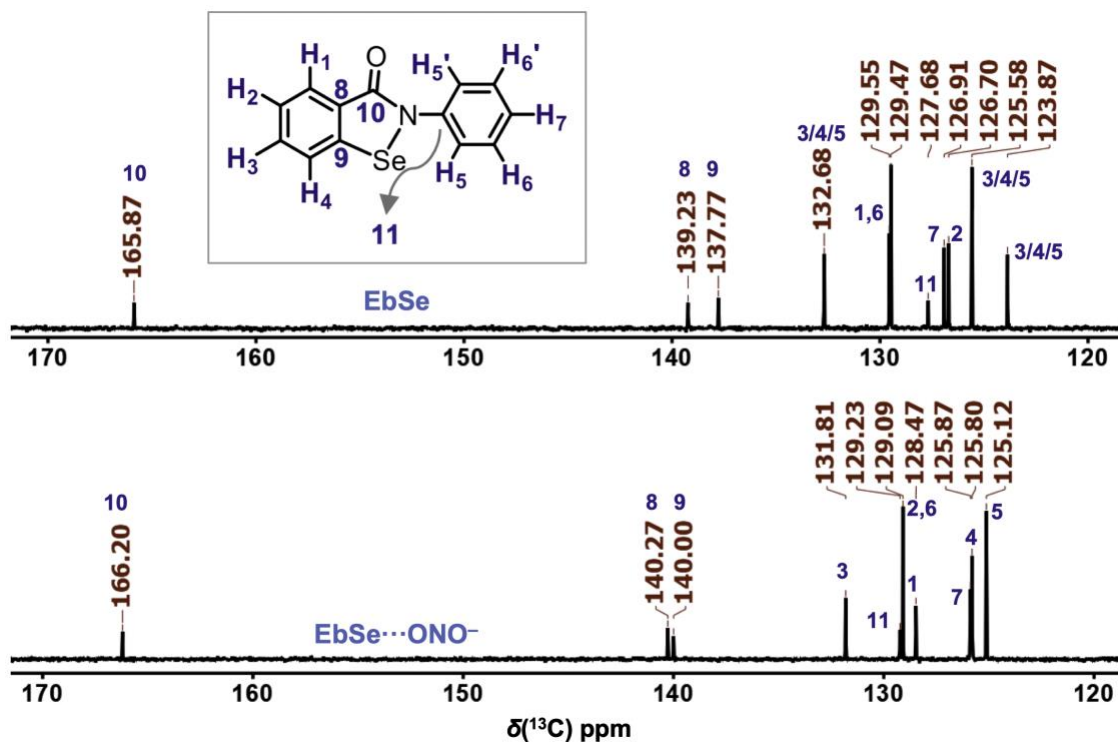
Figure S3. $^{13}C\{^{1}H\}$ NMR (125 MHz, CDCl₃) of **EbSe** (top) and **EbSe···ONO⁻** (bottom). The NMR sample was prepared by dissolving **EbSe** (0.010 g, 0.036 mmol) and [Bu₄N][NO₂] (0.010 g, 0.036 mmol) in CDCl₃. The aliphatic region of the bottom spectrum shows ^{13}C resonances for the Bu₄N⁺ and is not shown for clarity. The numbering scheme used for assigning the peaks is shown as inset.
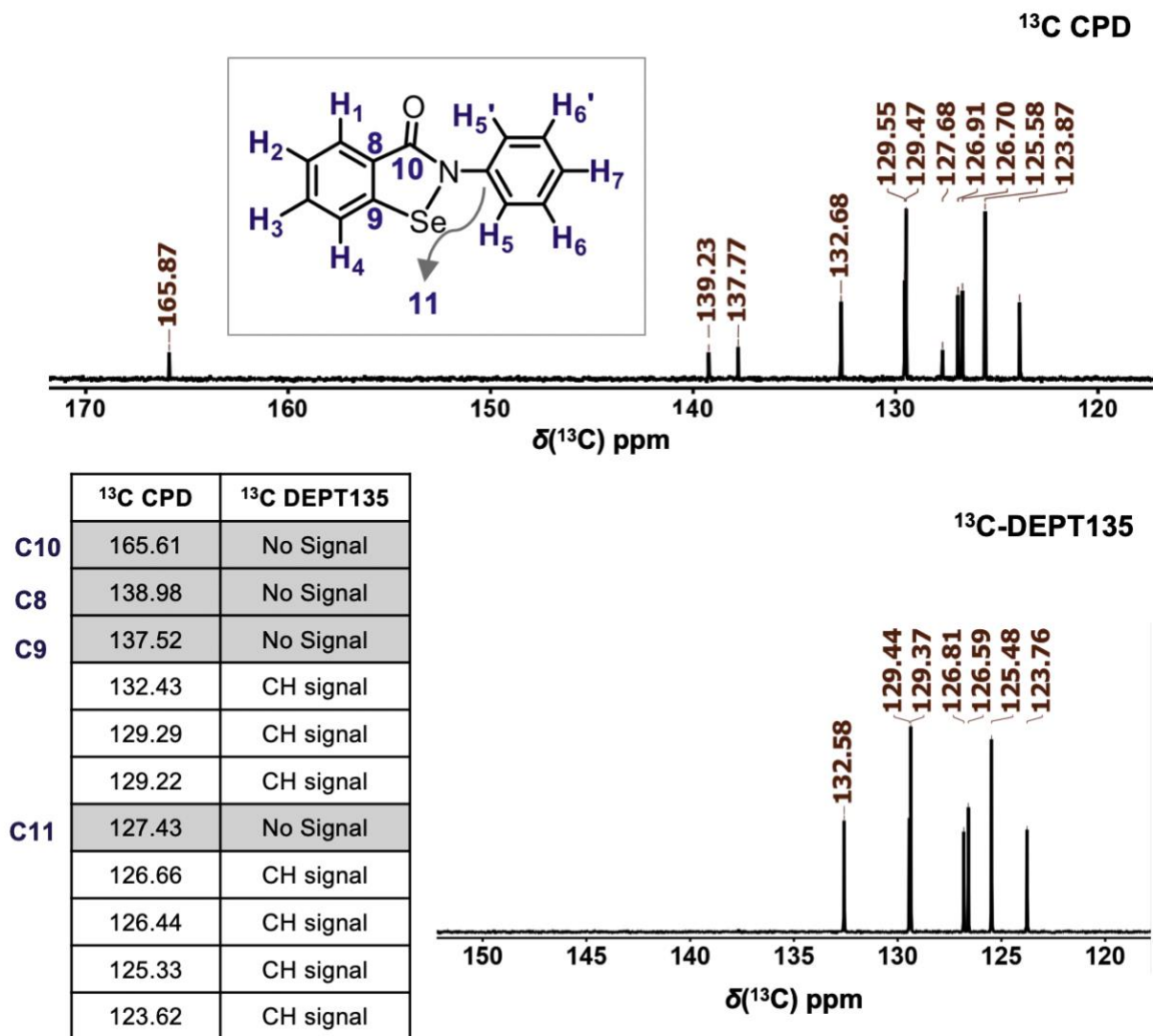
	^{13}C CPD	^{13}C DEPT135
C10	165.61	No Signal
C8	138.98	No Signal
C9	137.52	No Signal
	132.43	CH signal
	129.29	CH signal
	129.22	CH signal
C11	127.43	No Signal
	126.66	CH signal
	126.44	CH signal
	125.33	CH signal
	123.62	CH signal

Figure S4. Comparison of ^{13}C{^{1}H} NMR (top) and ^{13}C-DEPT135 (bottom) spectra of **EbSe** in CDCl$_3$. The identified signals for CH- and the tertiary carbon are listed in the table in the left corner.
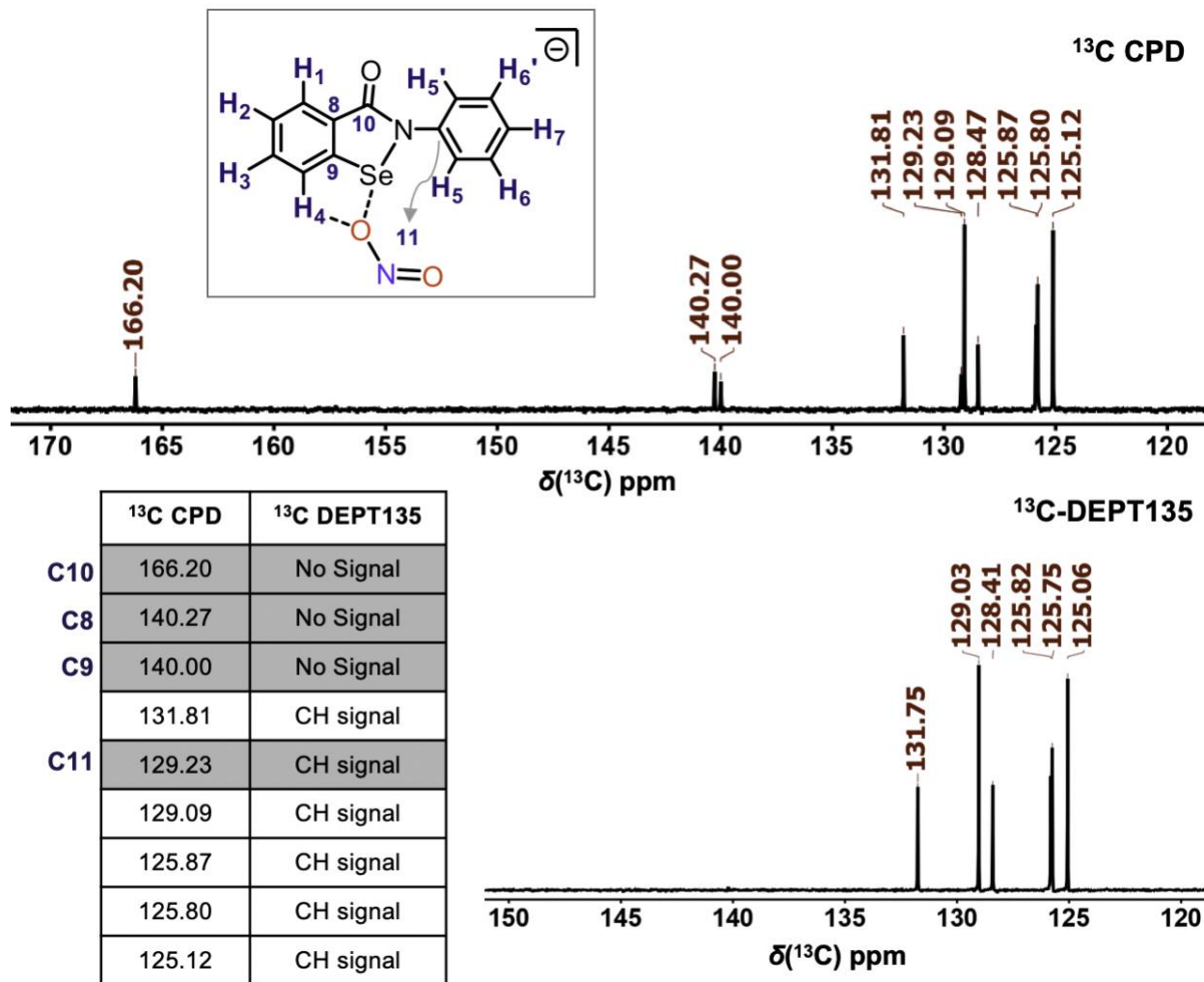
	^{13}C CPD	^{13}C DEPT135
C10	166.20	No Signal
C8	140.27	No Signal
C9	140.00	No Signal
	131.81	CH signal
C11	129.23	CH signal
	129.09	CH signal
	125.87	CH signal
	125.80	CH signal
	125.12	CH signal

Figure S5. Comparison of ^{13}C{^{1}H} NMR (top) and ^{13}C-DEPT135 (bottom) spectra of **EbSe⋯ONO$^-$** in CDCl$_3$. The identified signals for CH- and the tertiary carbon are listed in the table in the left corner. The numbering scheme used for assigning the peaks is shown as inset.
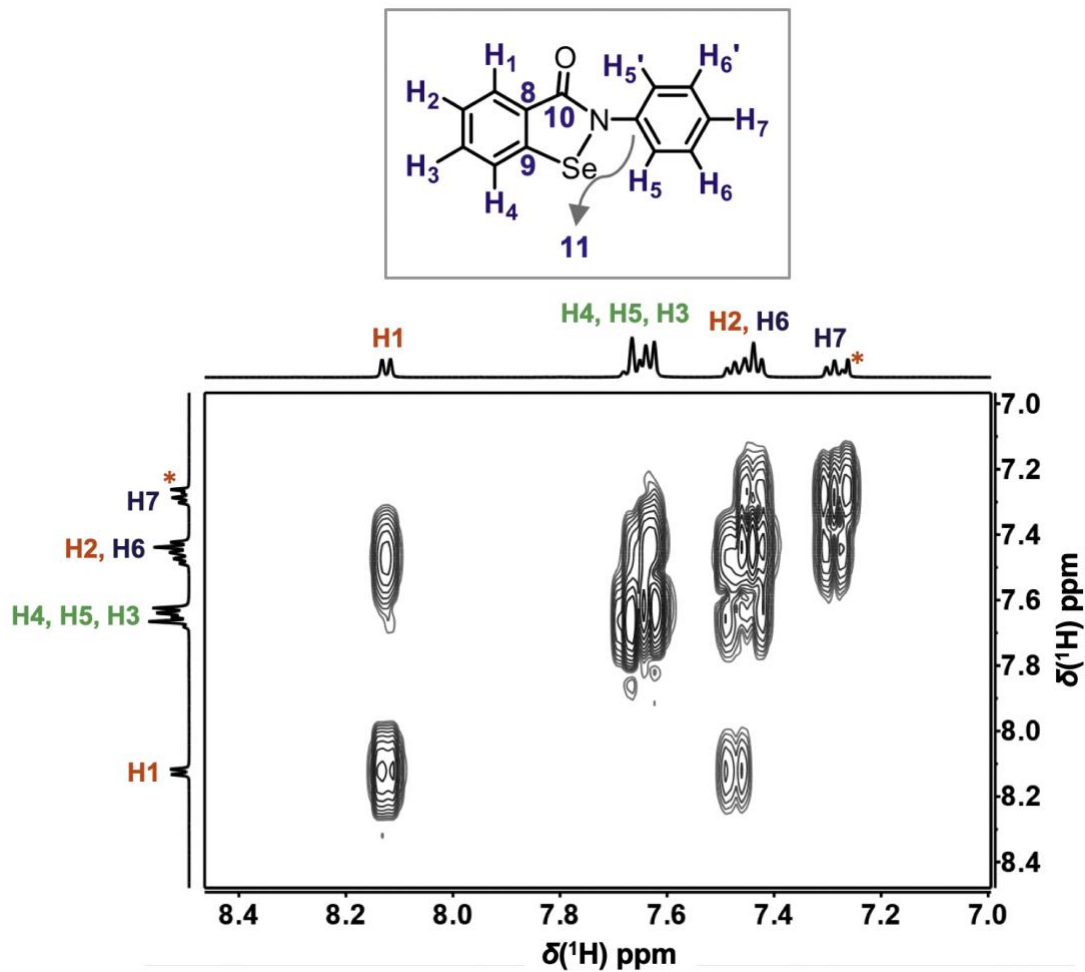
Figure S6. ¹H-¹H COSY spectrum (500 MHz, 298 K, in CDCl₃) of **EbSe**. The peak marked with * originates from the solvent residual peak of CDCl₃.
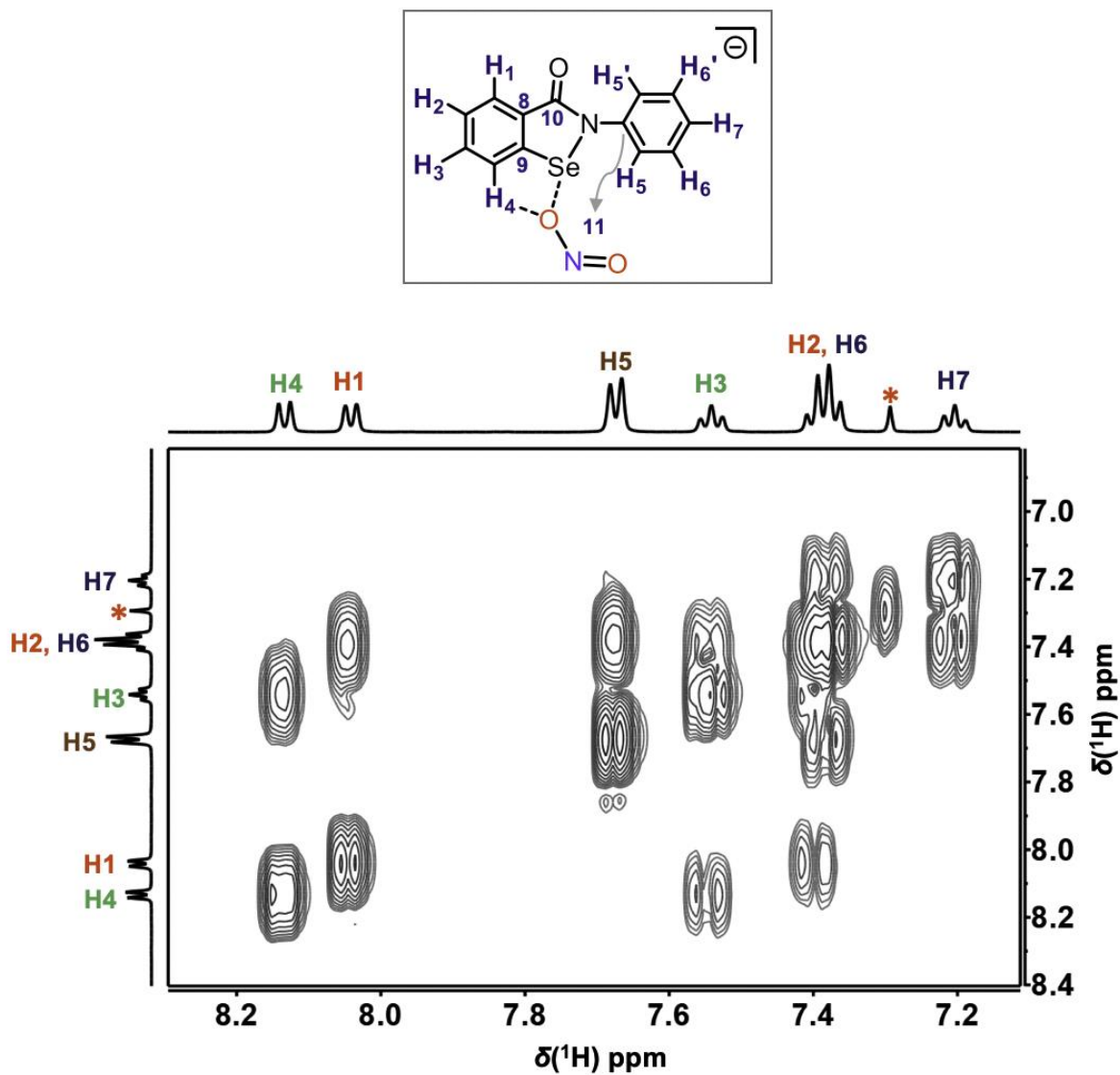
Figure S7. ^{1}H-^{1}H COSY spectrum (500 MHz, 298 K, in CDCl$_3$) of **EbSe···ONO^{-}**. The peak marked with * originates from the solvent residual peak of CDCl$_3$.

Comment: Nitrite anion in the adduct complex could alternatively interact with the H5–C5 site of **EbSe** while being engaged in the Se···O interaction. However, the chemical environment of the H5–C5 remains nearly unchanged upon the coordination of nitrite anion as suggested by the comparison of ^{1}H NMR spectra of **EbSe** and **EbSe···ONO^{-}** (Figures 4 and S7).
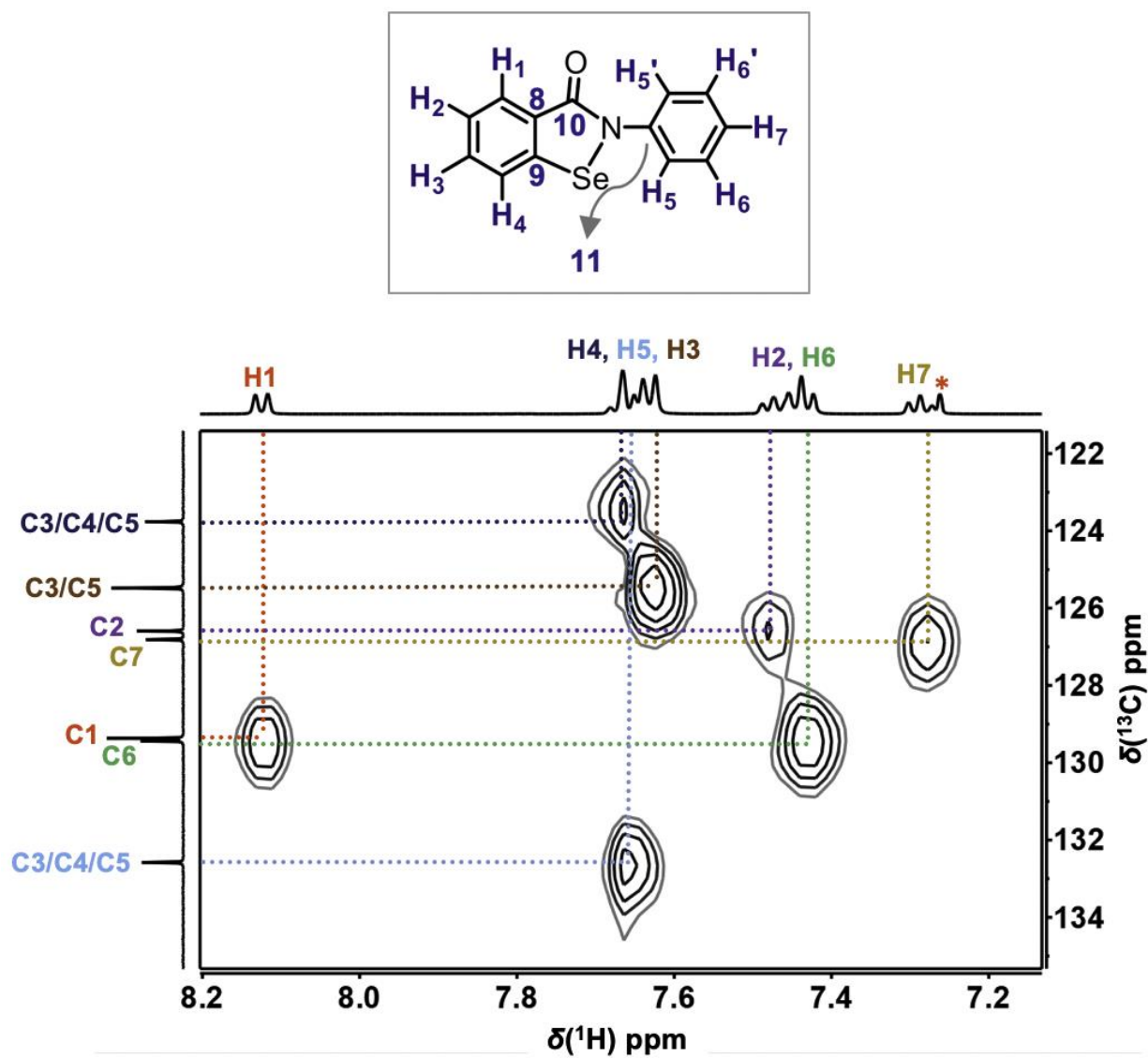
Figure S8. ^{13}C-^1H HMQC spectrum (500 MHz, 298 K, in $CDCl_3$) of **EbSe**.
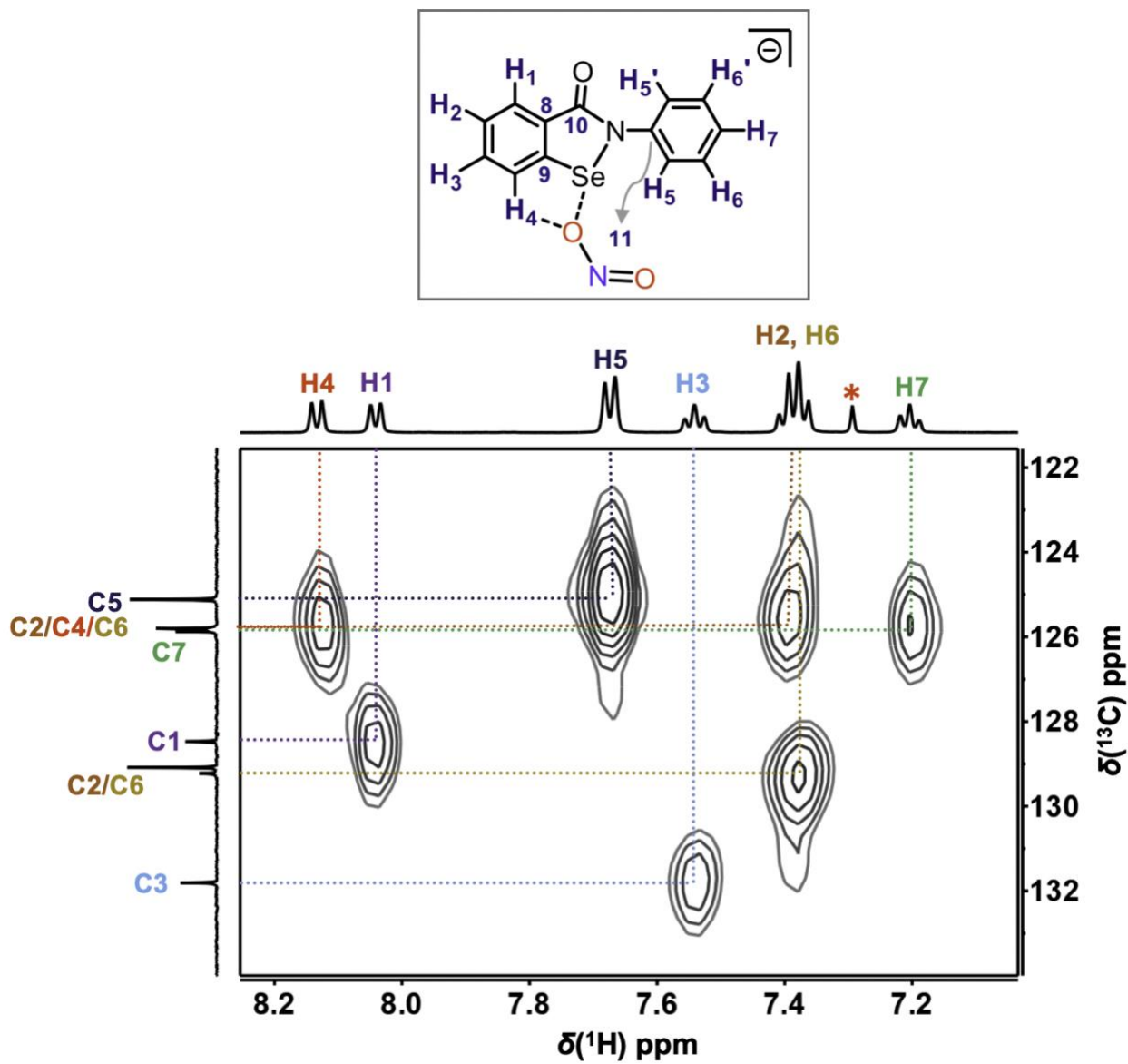
Figure S9. ^{13}C-^{1}H HMQC spectrum (500 MHz, 298 K, in CDCl$_3$) of **EbSe···ONO⁻**.
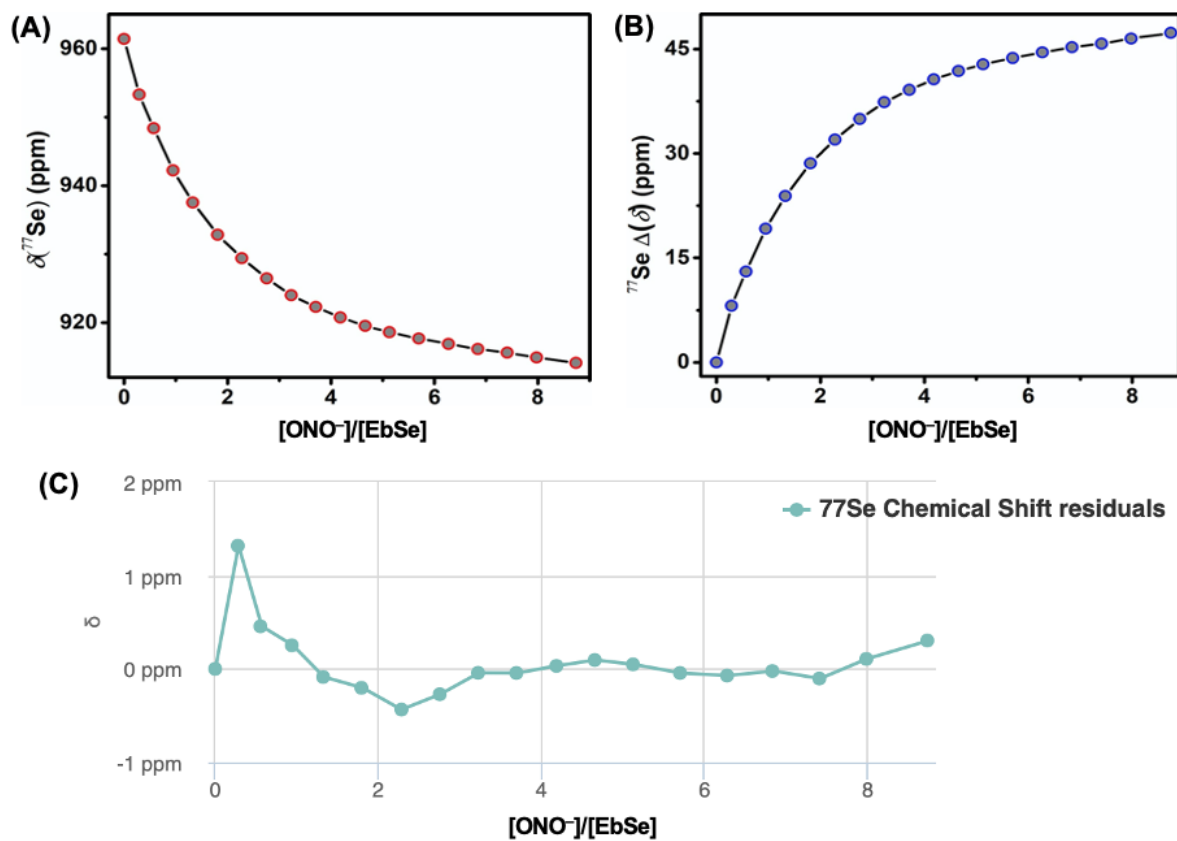
Figure S10. **(A)** The plot of ^{77}Se chemical shifts (δ, ppm) of **EbSe** versus [ONO$^-$]/[**EbSe**] ratio in CDCl$_3$ at room temperature. **(B)** Plot of $\Delta\delta$ of ^{77}Se of **EbSe** in CDCl$_3$ upon addition of incremental amounts of [Bu$_4$N][NO$_2$] ($\Delta\delta = \delta_0 - \delta_i$, where δ_0 = the chemical shift of a solution of authentic ebselen and δ_i = the chemical shift of a solution consisting of Ebselen along with i-th aliquot of nitrite anion). **(C)** ^{77}Se chemical shift residual from the fit to obtain the binding affinity. The corresponding ^{77}Se NMR spectra are shown as Figure 3.
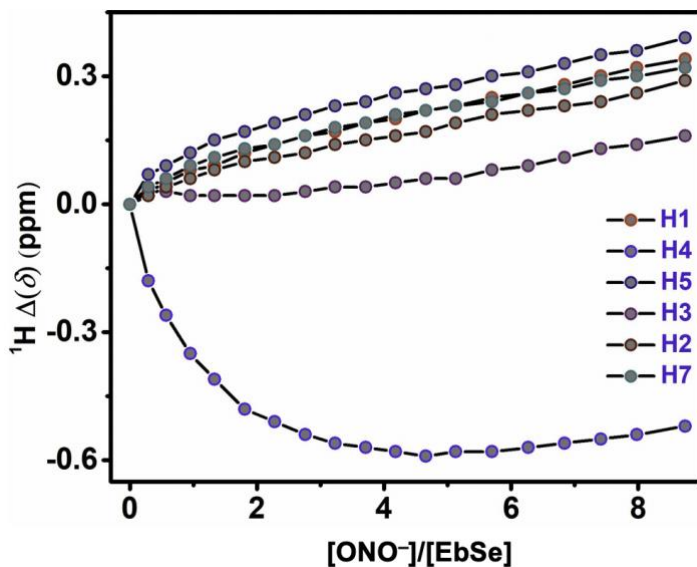
Figure S11. The plot of ^1H chemical shifts (δ, ppm) of **EbSe** versus [ONO$^-$]/[**EbSe**] ratio in CDCl$_3$ at room temperature. The corresponding ^1H NMR spectra are shown as Figure 4.

Figure S12. ^{77}Se NMR (95 MHz, CDCl$_3$) spectra of **EbSe** at room temperature upon increasing the ratio of nitrate anion and **EbSe** from 0.00 to 6.39 (as shown on the left panel).
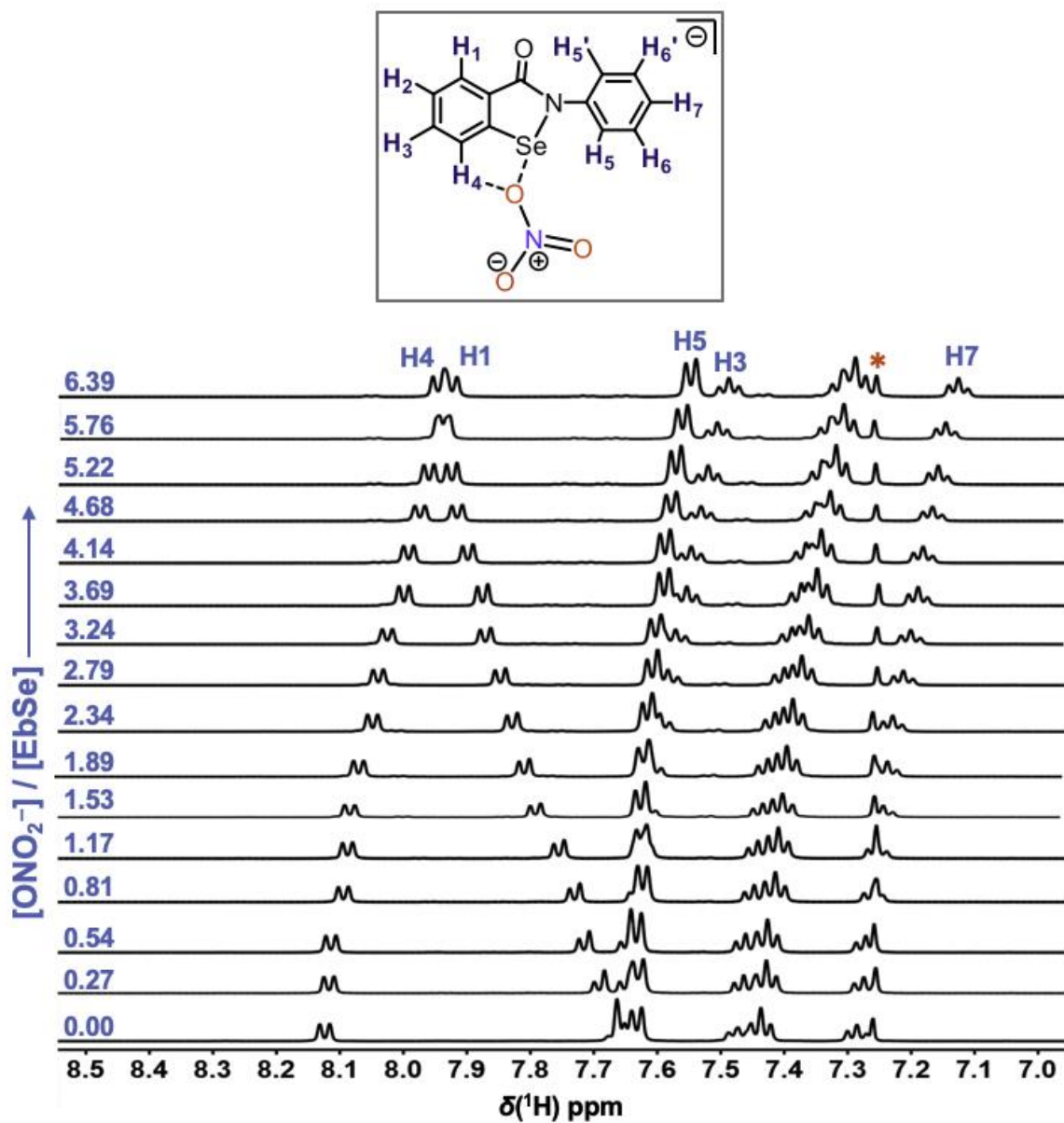
Figure S13. ^{1}H NMR (500 MHz, CDCl$_3$) spectra of **EbSe** at room temperature upon increasing the ratio of nitrate anion and **EbSe** from 0.00 to 6.39 (as shown on the left panel).
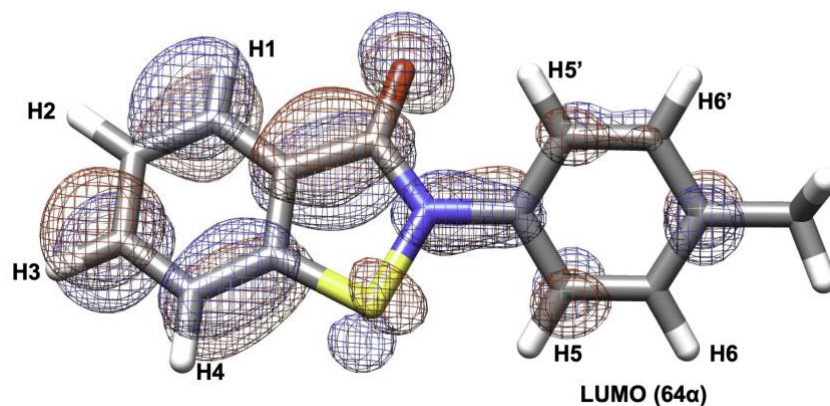
Figure S14. LUMO of **EbS** calculated at B3PW91/6- 311G(2df,p) level of theory.
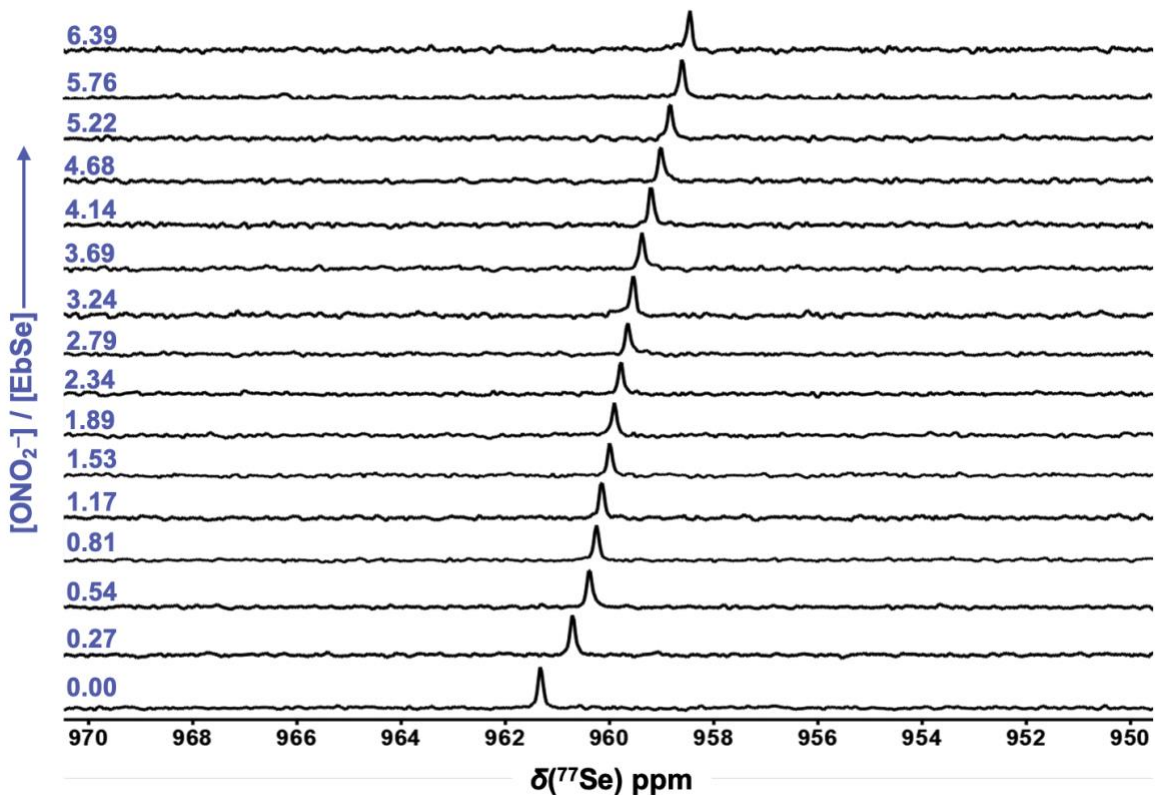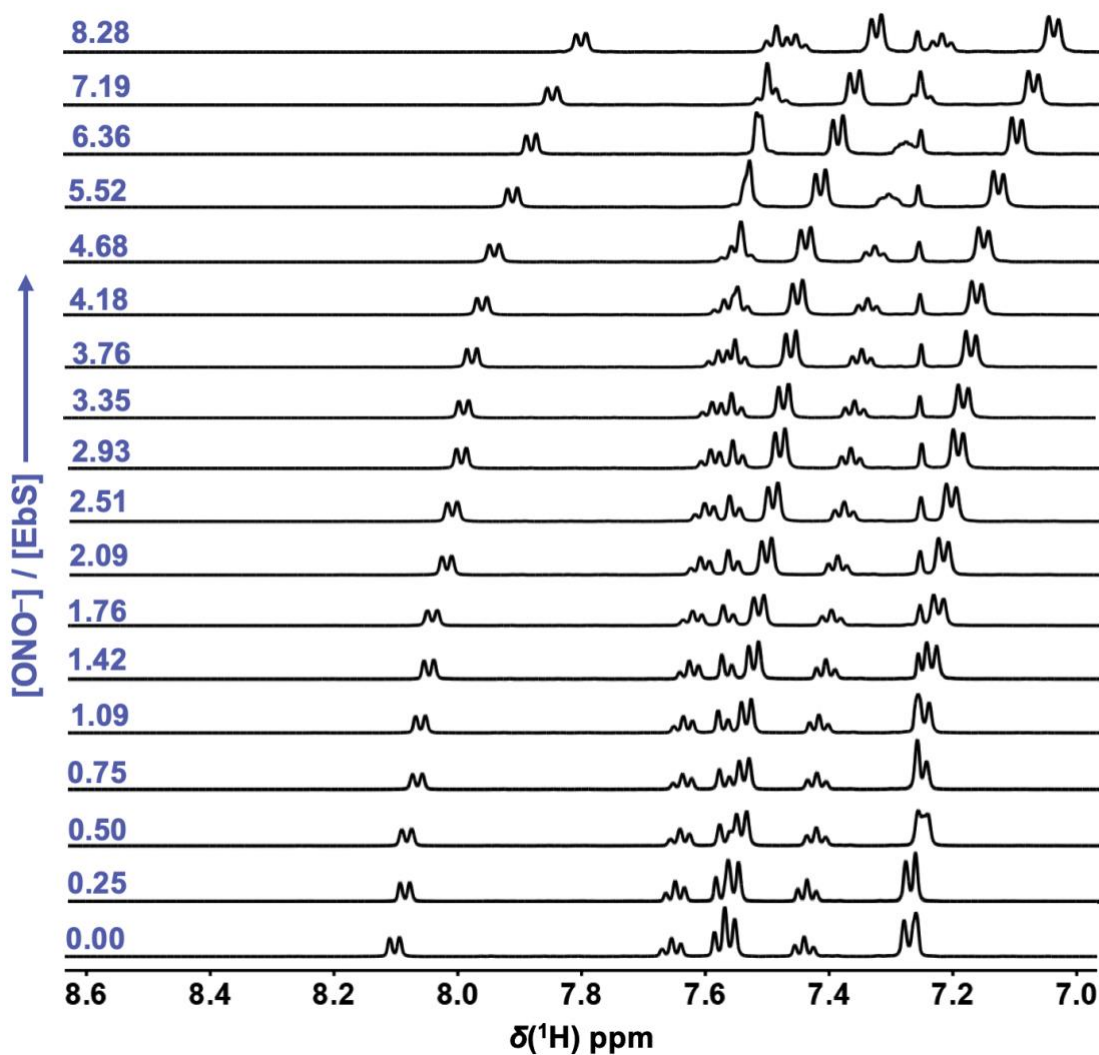

Figure S15. ^{1}H NMR (500 MHz, CDCl$_3$) spectra of **EbS** at room temperature upon increasing the ratio of nitrate anion and **EbS** from 0.00 to 8.28 (as shown on the left panel).
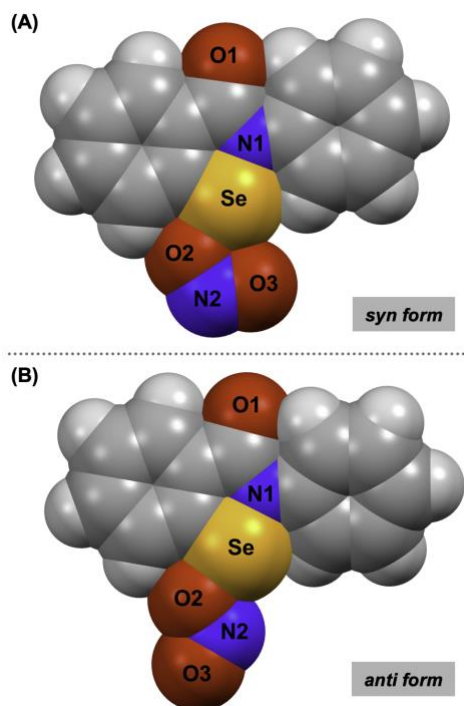
Figure S16. Space-filling models of the geometry-optimized structures of the syn **(A)** and anti **(B)** forms of **EbSe···ONO⁻** adducts at B3PW91/6- 311G(2df,p) level of theory.

Se···N1 1.990 Å
Se···O2 2.295 Å
O2···H4 2.158 Å
N1–Se···O2 170.19°
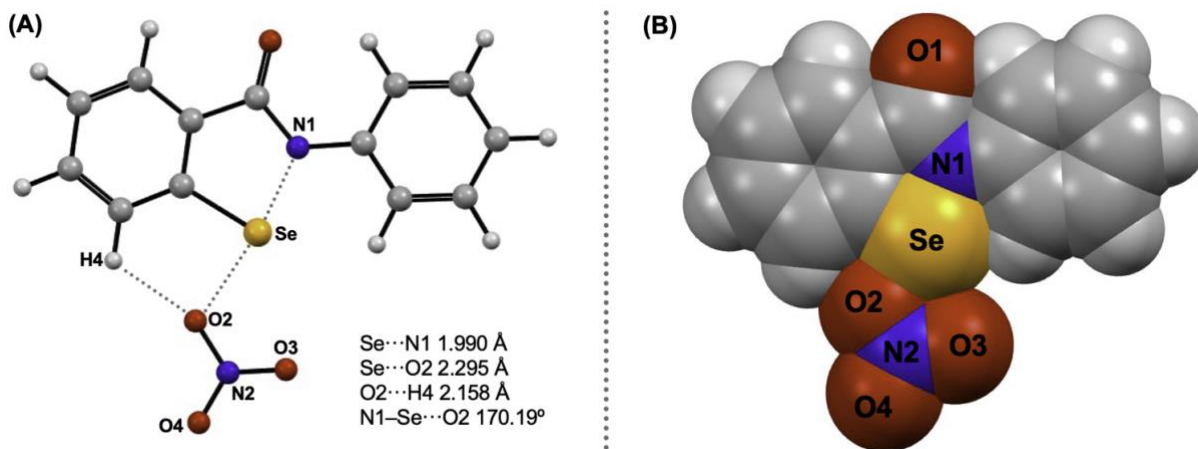
Figure S17. (A) Geometry-optimized structure of the **EbSe···ONO₂⁻** at B3PW91/6- 311G(2df,p) level of theory and **(B)** the corresponding space-filling model.
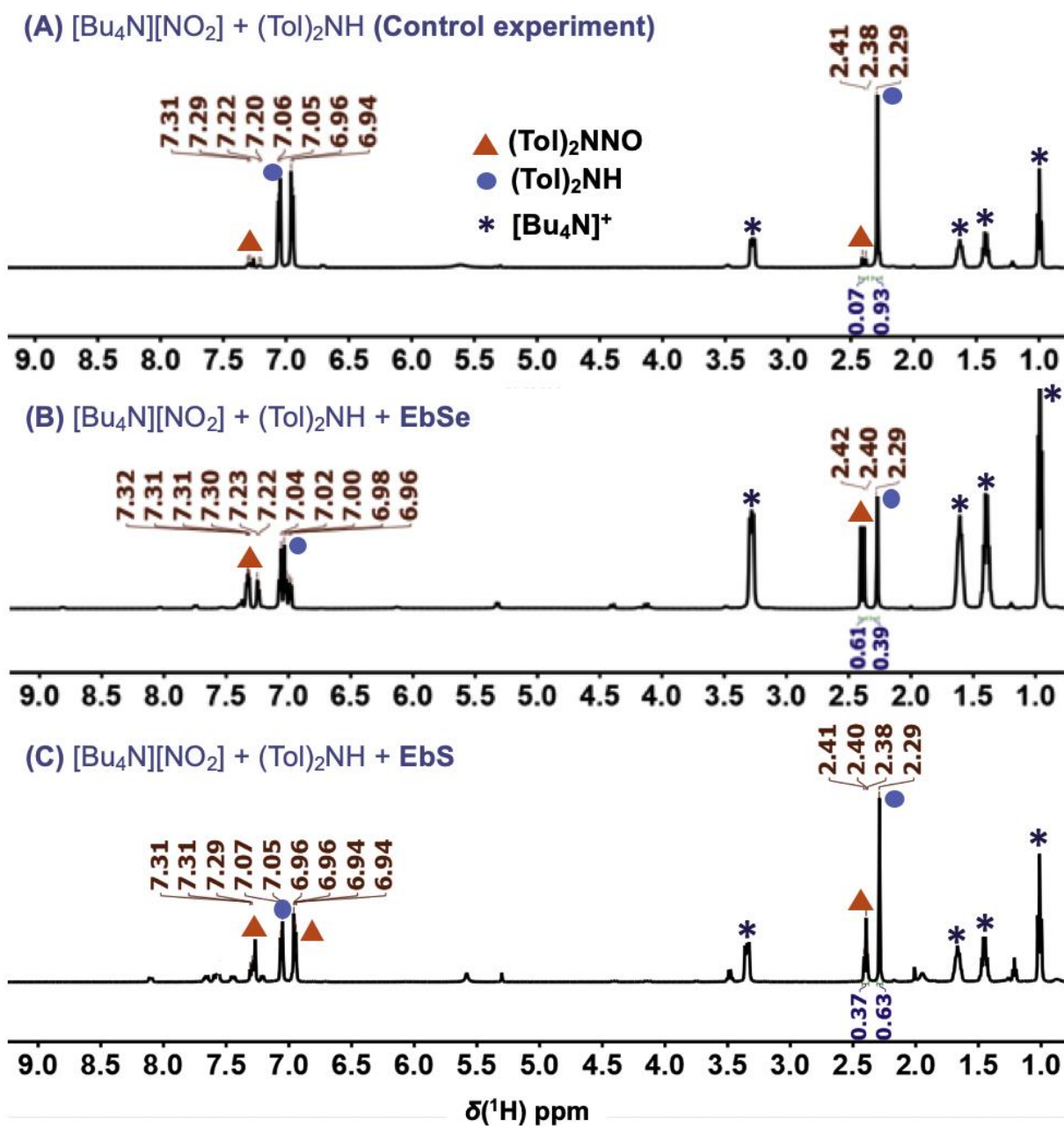
Figure S18. ^{1}H NMR (500 MHz, CDCl3) spectra of the crude reaction mixtures as obtained from the reactions of (*p*-tolyl)2NH and [Bu4N][ONO] in the presence of a stoichiometric amount of **EbSe/EbS** (as indicated above).
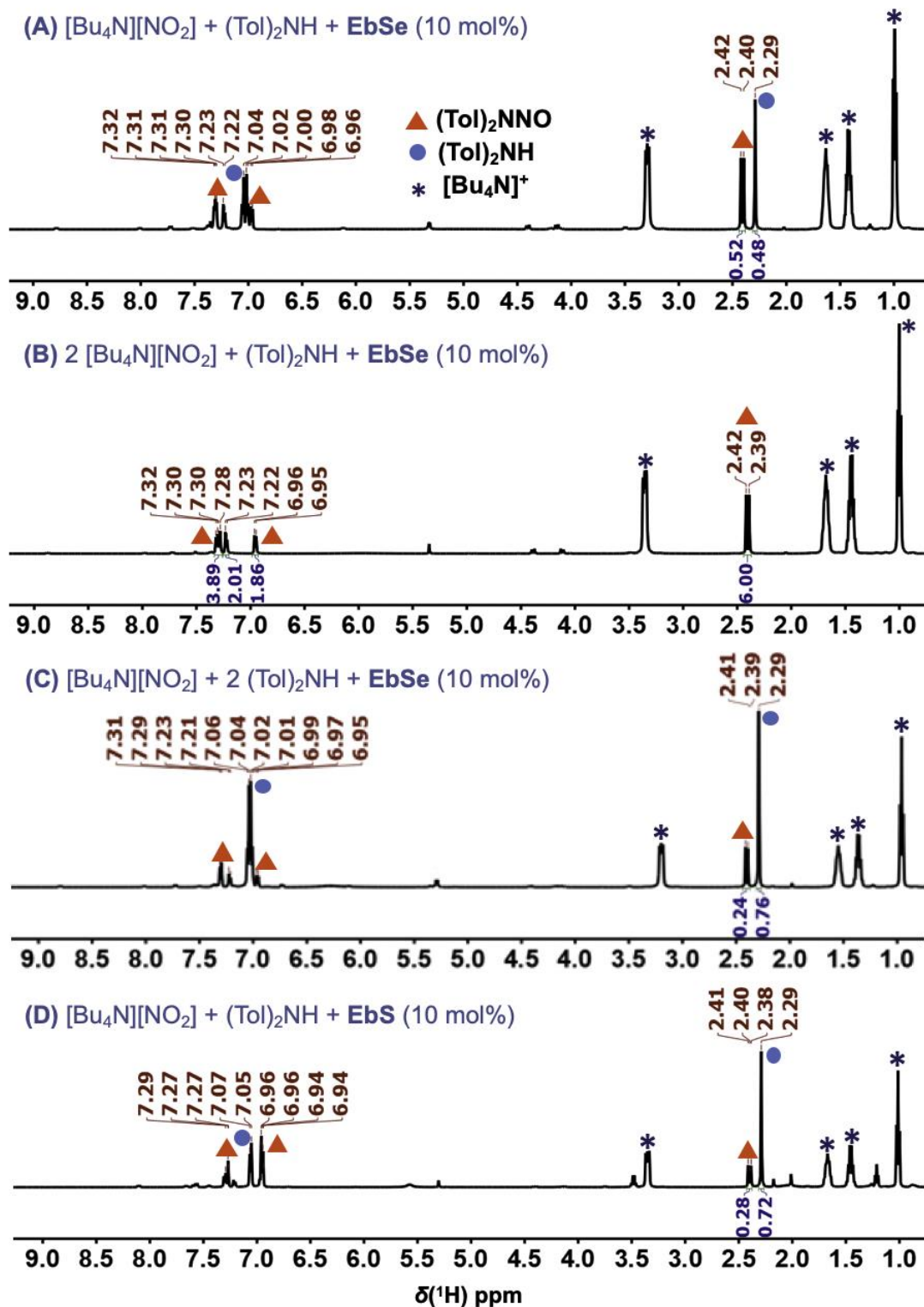
Figure S19. ^{1}H NMR (500 MHz, CDCl$_3$) spectra of the crude reaction mixtures as obtained from the reactions of (*p*-tolyl)$_2$NH and [Bu$_4$N][ONO] in the presence of a catalytic amount of **EbSe/EbS** (as indicated above).
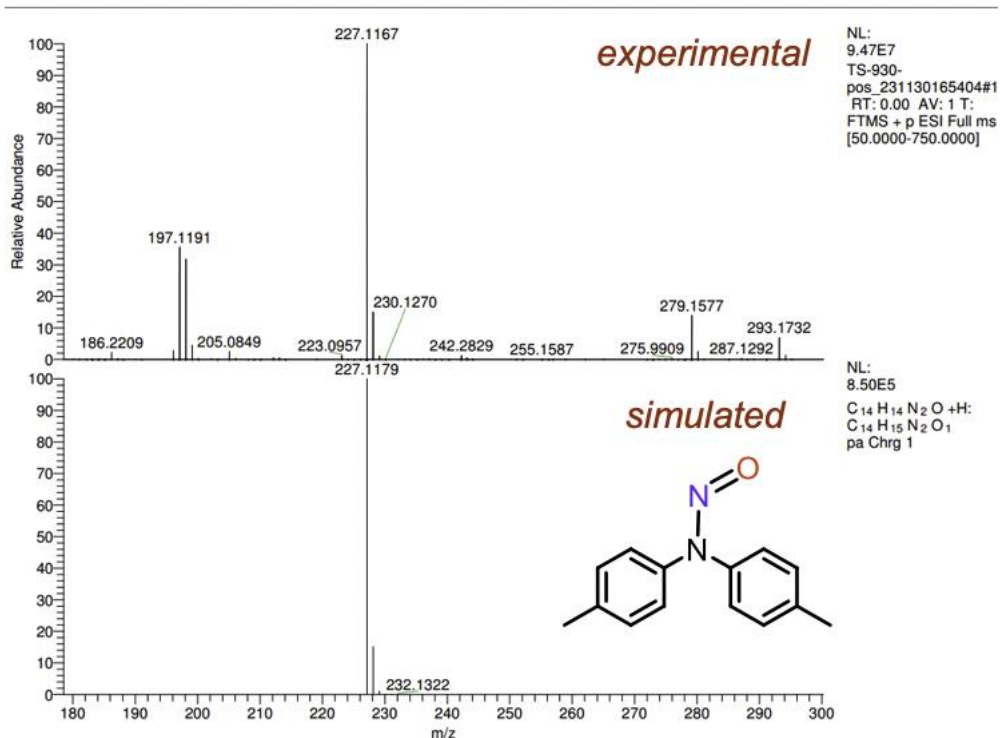
Figure S20. HRMS (ESI+) spectrum of the crude reaction mixtures as obtained from the reactions of (*p*-tolyl)$_2$NH and [Bu$_4$N][ONO] in the presence of a stoichiometric amount of **EbSe**.
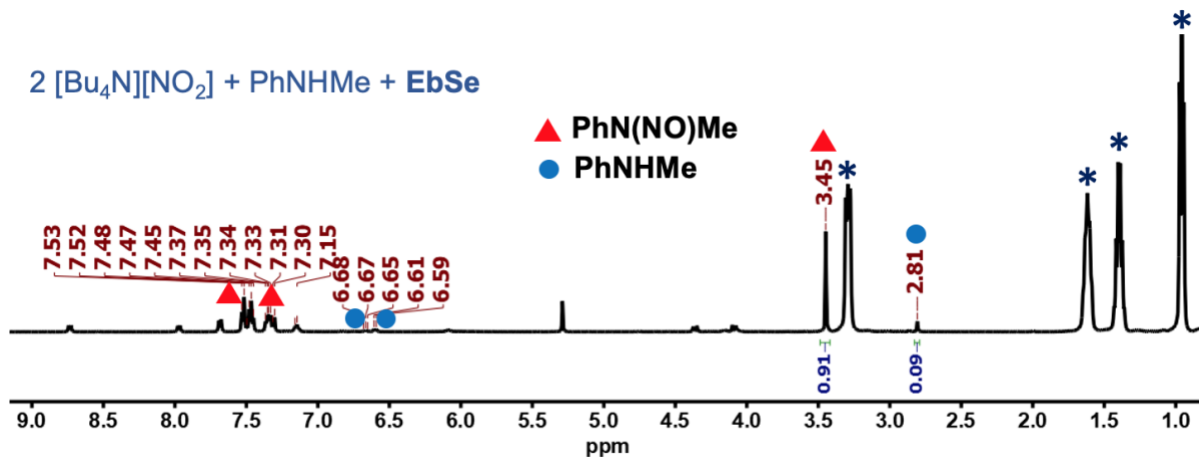
Figure S21. ^{1}H NMR (500 MHz, CDCl$_3$) spectrum of the crude reaction mixtures as obtained from the reactions of *N*-methylphenylamine and [Bu$_4$N][NO$_2$] in the presence of **EbSe** (as indicated above). The chemical shifts are assigned as reported elsewhere.[S11]

Figure S22. ^{31}P NMR (202 MHz, CDCl$_3$, 298 K) spectra of triethylphosphine oxide (top) and upon addition of one equiv. of **EbSe** to that (bottom).

7.   Tables

Table S1. Details of the amount of [Bu₄N][NOₓ] (x=2/3) used and the corresponding concentrations and the ratio [NOₓ⁻]/[**EbSe**] for the ^{77}Se and ^{1}H NMR titration experiments.

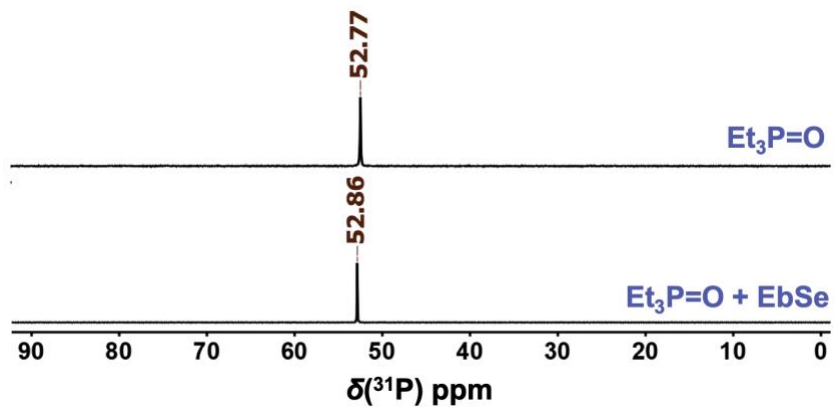|	[Bu₄N][NO₂] weight	[NO₂⁻]	[NO₂⁻]/[EbSe]		[Bu₄N][NO₃] Weight	[NO₃⁻]	[NO₂⁻]/[EbSe]
Vial 1	3 mg	10.40 mM	0.29	**Vial 1**	3 mg	9.85 mM	0.27
Vial 2	3 mg	20.80 mM	0.57	**Vial 2**	3 mg	19.71 mM	0.54
Vial 3	4 mg	34.67 mM	0.95	**Vial 3**	3 mg	29.56 mM	0.81
Vial 4	4 mg	48.53 mM	1.33	**Vial 4**	4 mg	42.70 mM	1.17
Vial 5	5 mg	65.86 mM	1.81	**Vial 5**	4 mg	55.83 mM	1.53
Vial 6	5 mg	83.20 mM	2.28	**Vial 6**	4 mg	68.97 mM	1.89
Vial 7	5 mg	100.53 mM	2.76	**Vial 7**	5 mg	85.39 mM	2.34
Vial 8	5 mg	117.86 mM	3.23	**Vial 8**	5 mg	101.82 mM	2.79
Vial 9	5 mg	135.20 mM	3.71	**Vial 9**	5 mg	118.24 mM	3.24
Vial 10	5 mg	152.53 mM	4.18	**Vial 10**	5 mg	134.66 mM	3.69
Vial 11	5 mg	169.86 mM	4.66	**Vial 11**	6 mg	151.08 mM	4.14
Vial 12	5 mg	187.19 mM	5.13	**Vial 12**	6 mg	170.79 mM	4.68
Vial 13	6 mg	207.99 mM	5.70	**Vial 13**	6 mg	190.49 mM	5.22
Vial 14	6 mg	228.79 mM	6.27	**Vial 14**	6 mg	210.20 mM	5.76
Vial 15	6 mg	249.59 mM	6.84	**Vial 15**	7 mg	233.19 mM	6.39
Vial 16	6 mg	270.39 mM	7.41				
Vial 17	6 mg	291.19 mM	7.98				
Vial 18	8 mg	318.92 mM	8.74				

Table S2. Selected distances obtained from the DFT optimised structures of **EbSe** and their corresponding adduct complexes with NOₓ⁻ (x = 2,3) anions. The last column represents the change of Gibbs free energy (ΔG) for the adduct forming reaction: **EbSe + NOₓ⁻ = EbSe···ONOₓ₋₁⁻**.

	Se–N1	Se–C9	Se–O2	O2–H4	ΔG (kcal/mol)
EbSe	1.875 (1.880) Å	1.880 (1.878) Å	---	---	---
EbSe···ONO⁻ (*syn*)	2.089 (2.022) Å	1.898 (1.902) Å	2.211 (2.275) Å	2.159 (2.176) Å	–34.55 (–10.96)
EbSe···ONO⁻ (*anti*)	2.043 Å	1.890 Å	2.168 Å	2.167 Å	–32.37
EbSe···ONO₂⁻	1.990 (1.947) Å	1.890 (1.894) Å	2.295 (2.397) Å	2.158 (2.194) Å	–22.30 (–2.57)
B3PW91/6-311G(2df,p) level of DFT and the values in the solvent phase (SMD, Chloroform) are given in the parentheses					

Table S3. Geometry optimized coordinates of **EbSe** and **EbS** at B3PW91/6-311G(2df,p) level of theory.

EbSe				EbS			
C	1.7585	0.8453	0.1061	C	2.2296	0.6078	0.0756
C	2.0132	-0.5158	-0.0654	C	2.3594	-0.7648	-0.1022
C	3.3154	-1.0107	-0.1226	C	3.6115	-1.3677	-0.169
C	4.3665	-0.1061	-0.0036	C	4.726	-0.5559	-0.0515
C	4.1254	1.2634	0.1711	C	4.6062	0.8252	0.1306
C	2.8228	1.7418	0.2269	C	3.3571	1.4121	0.1952
C	0.3368	1.2556	0.1556	C	0.8407	1.0737	0.1237
H	3.5125	-2.068	-0.2554	H	3.716	-2.4374	-0.3079
H	5.3866	-0.471	-0.0464	H	5.7122	-1.0042	-0.1013
H	4.9598	1.9485	0.2627	H	5.4987	1.4332	0.2205
H	2.6038	2.7946	0.3624	H	3.2264	2.479	0.3364
N	-0.4961	0.1451	0.0258	N	0.0022	-0.0332	-0.0251
O	-0.0683	2.3974	0.2975	O	0.4569	2.2154	0.2729
C	-1.9179	0.1833	0.0308	C	-1.4108	-0.0142	-0.0067
C	-2.6365	-0.8049	0.7117	C	-2.1157	-1.1321	0.4302
C	-2.6042	1.1932	-0.6533	C	-2.1182	1.1075	-0.4413
C	-4.0287	-0.7906	0.6996	C	-3.5017	-1.1312	0.4257
H	-2.1061	-1.5738	1.2621	H	-1.5828	-2.0053	0.7897
C	-3.9957	1.2069	-0.6438	C	-3.5012	1.0918	-0.4249
H	-2.0495	1.9645	-1.1678	H	-1.5813	1.9836	-0.7722
C	-4.7145	0.2166	0.0246	C	-4.2239	-0.0206	0.0041
H	-4.5747	-1.563	1.2292	H	-4.029	-2.0162	0.7674
H	-4.52	1.996	-1.1709	H	-4.0343	1.9743	-0.7656
H	-5.7981	0.2314	0.0208	S	0.8103	-1.5404	-0.2216
Se	0.3987	-1.5154	-0.2024	C	-5.7248	-0.0074	0.0236
				H	-6.1037	0.6274	0.8311
				H	-6.1322	0.3848	-0.9117
				H	-6.1306	-1.0093	0.1739

TableS4. Geometry optimized coordinates of the syn and anti forms of **EbSe···ONO⁻** at B3PW91/6-311G(2df,p) level of theory.

EbSe···ONO⁻ (syn)				EbSe···ONO⁻ (anti)			
C	3.4265	-2.7461	0.0000	C	2.9995	-3.1428	0.0859
C	2.0452	-2.8888	0.0000	C	1.6111	-3.1282	0.1029
C	1.2246	-1.7576	0.0000	C	0.9262	-1.9108	0.0607
C	3.9863	-1.4623	0.0000	C	3.7034	-1.9326	0.0254
C	3.1831	-0.3258	0.0000	C	3.0374	-0.7118	-0.0168
C	1.7905	-0.4756	0.0000	C	1.6371	-0.7047	0.0023
C	-0.2571	-1.8797	0.0000	C	-0.5569	-1.8462	0.0758
N	-0.8433	-0.6449	0.0000	N	-0.9764	-0.5435	0.0582
Se	0.5086	0.9493	0.0000	Se	0.5307	0.8509	-0.0481
C	-2.2221	-0.3975	0.0000	C	-2.3171	-0.1329	0.0416
C	-3.1985	-1.4187	0.0001	C	-3.3639	-0.9552	-0.4228
C	-4.5541	-1.0997	0.0002	C	-4.6721	-0.4807	-0.4479
C	-2.6771	0.9385	-0.0002	C	-2.6414	1.1657	0.4785
C	-4.034	1.2387	-0.0002	C	-3.9527	1.6282	0.4419
C	-4.9905	0.2238	0.0000	C	-4.9824	0.8104	-0.0212
H	4.0679	-3.6211	0.0000	H	3.5375	-4.0845	0.1184
H	1.5672	-3.8619	-0.0001	H	1.0266	-4.0403	0.1488
H	5.0656	-1.344	0.0000	H	4.7889	-1.9405	0.0106
H	3.6171	0.6636	0.0001	H	3.579	0.2225	-0.0652
O	-0.8259	-2.979	-0.0001	O	-1.2734	-2.853	0.1116
H	-2.8727	-2.4466	0.0003	H	-3.1369	-1.9613	-0.7399
H	-5.2788	-1.9086	0.0003	H	-5.4596	-1.1349	-0.8096
H	-6.0492	0.4603	0.0000	H	-6.0053	1.1706	-0.0463
H	-1.9646	1.7536	-0.0004	H	-1.8591	1.8096	0.8607
H	-4.3412	2.2796	-0.0003	H	-4.1674	2.6353	0.7846
N	2.0172	3.6524	0.0001	N	2.0868	3.3377	-0.0162
O	2.2883	2.3955	0.0001	O	3.0205	4.1211	-0.092
O	0.8302	3.9587	-0.0001	O	2.4165	2.0925	-0.1894

Table S5. Geometry optimized coordinates of **EbSe···ONO₂⁻** at B3PW91/6-311G(2df,p) level of theory.

EbSe···ONO₂⁻			
C	-2.4942	3.6694	0.0648
C	-1.1174	3.4918	0.0821
C	-0.5849	2.2001	0.0485
C	-3.3376	2.5505	0.0145
C	-2.8232	1.2584	-0.0178
C	-1.4338	1.0881	-0.0007
C	0.8752	1.9481	0.0647
N	1.1289	0.5966	0.0383
Se	-0.5001	-0.5774	-0.0347
C	2.4069	0.0088	0.0285
C	3.5696	0.7202	-0.3296
C	4.8055	0.0799	-0.3487
C	2.54	-1.3521	0.3633
C	3.7814	-1.9782	0.334
C	4.9279	-1.2696	-0.0211
H	-2.9172	4.668	0.0903
H	-0.4295	4.3289	0.1216
H	-4.4142	2.6884	0.0008
H	-3.4736	0.3956	-0.055
O	1.7174	2.8492	0.1041
H	3.4889	1.768	-0.5719
H	5.6853	0.6516	-0.6277
H	5.8958	-1.7588	-0.0411
H	1.6688	-1.9248	0.6565
H	3.8464	-3.0292	0.5952
N	-2.6006	-2.9194	-0.0556
O	-2.6354	-1.6265	-0.1376
O	-1.5001	-3.4885	0.0443
O	-3.6742	-3.5326	-0.0813

Table S5. Geometry optimized coordinates of nitrite and nitrate anions at B3PW91/6-311G(2df,p) level of theory.

ONO⁻				ONO₂⁻			
N	0.0000	0.0000	0.4587	N	0.0000	0.0000	-0.0001
O	0.0000	1.0710	-0.2007	O	0.5042	-1.1547	0.0000
O	0.0000	-1.0710	-0.2007	O	0.7479	1.0140	0.0000
				O	-1.2521	0.1407	0.0000

8. References

S1. Gaussian 16, Revision C.01, Frisch, M. J.; Trucks, G. W.; Schlegel, H. B.; Scuseria, G. E.; Robb, M. A.; Cheeseman, J. R.; Scalmani, G.; Barone, V.; Petersson, G. A.; Nakatsuji, H.; Li, X.; Caricato, M.; Marenich, A. V.; Bloino, J.; Janesko, B. G.; Gomperts, R.; Mennucci, B.; Hratchian, H. P.; Ortiz, J. V.; Izmaylov, A. F.; Sonnenberg, J. L.; Williams-Young, D.; Ding, F.; Lipparini, F.; Egidi, F.; Goings, J.; Peng, B.; Petrone, A.; Henderson, T.; Ranasinghe, D.; Zakrzewski, V. G.; Gao, J.; Rega, N.; Zheng, G.; Liang, W.; Hada, M.; Ehara, M.; Toyota, K.; Fukuda, R.; Hasegawa, J.; Ishida, M.; Nakajima, T.; Honda, Y.; Kitao, O.; Nakai, H.; Vreven, T.; Throssell, K.; Montgomery, J. A., Jr.; Peralta, J. E.; Ogliaro, F.; Bearpark, M. J.; Heyd, J. J.; Brothers, E. N.; Kudin, K. N.; Staroverov, V. N.; Keith, T. A.; Kobayashi, R.; Normand, J.; Raghavachari, K.; Rendell, A. P.; Burant, J. C.; Iyengar, S. S.; Tomasi, J.; Cossi, M.; Millam, J. M.; Klene, M.; Adamo, C.; Cammi, R.; Ochterski, J. W.; Martin, R. L.; Morokuma, K.; Farkas, O.; Foresman, J. B.; Fox, D. J. Gaussian, Inc., Wallingford CT, 2016.

S2. (a) J. P. Perdew, *Phys. Rev. B* **1986**, *34*, 7406-7406. (b) C. T. Lee, W. T. Yang, R. G. Parr, *Phys. Rev. B* **1988**, *37*, 785-789. (c) J. P. Perdew, *Phys. Rev. B* **1989**, *33*, 8822-8824.

S3. A. V. Marenich, C. J. Cramer and D. G. Truhlar, *J. Phys. Chem. B*, **2009**, *113*, 6378–6396.

S4. GaussView, Version 6, Dennington, Roy; Keith, Todd A.; Millam, John M. Semichem Inc., Shawnee Mission, KS, 2016.

S5. Avogadro: an open-source molecular builder and visualization tool. Version 1.2. http://avogadro.cc/

S6. CCDC Mercury Version 3.10; C. F. Macrae, P. R. Edgington, P. McCabe, E. Pidcock, G. P. Shields, R. Taylor, M. Towler, J. van de Streek, *J. Appl. Crystallogr.* **2006**, *39*, 453-457.

S7. (a) http://www.rbvi.ucsf.edu/chimera/1.9/docs/credits.html; (b) UCSF Chimera; E. F. Pettersen, T. D. Goddard, C. C. Huang, G. S. Couch, D. M. Greenblatt, E. C. Meng, T. E. Ferrin, *J. Comput. Chem.* **2004**, *25*, 1605-1612.

S8. A. V. Marenich, C. J. Cramer, D. G. Truhlar, *J. Phys. Chem. B* **2009**, *113*, 6378-6396.

S9. (a) B. Hibbert, D. P. Thordarson, *Chem. Commun.* **2016**, *52*, 12792-12805. (b) http://supramolecular.org.

S10. (a) M. S. Oderinde, N. H. Jones, A. Juneau, M. Frenette, B. Aquila, S. Tentarelli, D. W. Robbins, J. W. Johannes, *Angew. Chem. Int. Ed.* **2016**, *55*, 13219-13225. (b) X. Jia, P. Li, Y. Shao, Y. Yuan, H. Ji, W. Hou, X. Liu, X. Zhang, *Green Chem.*, **2017**, *19*, 5568-5574.

S11. (a) C. Wang, Y. Huang, *Org. Lett.* **2013**, *15*, 5294-5297. (b) O. Ogata, H. Nara, M. Fujiwhara, K. Matsumura, Y. Kayaki, *Org. Lett.* **2018**, *20*, 3866-3870.